Simultaneous Measurement of Strain and Temperature Using Liquid Core Optical Fiber Sensors
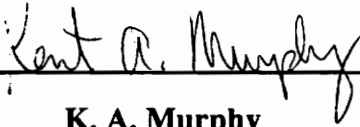
by: Marten Johannes Cornelius de Vries

Thesis submitted to the Faculty of the

Virginia Polytechnic Institute and State University

in partial fulfilment of the requirement for the degree of

Master of Science
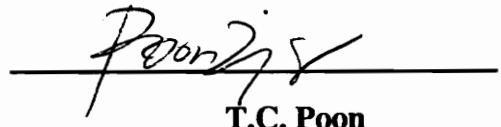
in

Electrical Engineering

APPROVED:

Richard O. Claus

R. O. Claus, Chairman

Kent A. Murphy   *Poon*

K. A. Murphy   T.C. Poon

January, 1993

Blacksburg, Virginia

Simultaneous Measurement of Strain and Temperature Using Liquid Core Optical Fiber Sensors

by

Marten J.C. de Vries

Richard O. Claus, Chairman

Electrical Engineering

(ABSTRACT)

A liquid core fiber sensor can be used to sense both strain and temperature simultaneously. This liquid core fiber sensor is comprised of a hollow core optical fiber filled with a liquid of a known index of refraction which is slightly higher than that of the silica tube which acts as the cladding. The refractive index fluid is chosen such that the variation of its refractive index with strain and temperature is well defined and linear in the desired range of operation. The core of the sensing fiber contains a fluid which has a thermo-optic coefficient much larger in magnitude ($-4.0 \times 10^{-4}/°C$) than that of the silica cladding. This causes the fiber to be more sensitive to temperature changes than all-silica fibers. Both transmitted optical signal intensity and time-of-flight depend strongly on applied strain and temperature. Furthermore, the relative difference between the core and cladding refractive indices changes as a function of both parameters due to the inherently different material types used in the fiber construction. This results in critical strain and temperature regimes within which the refractive index difference is very small, and sensitivity is optimized. Testing of prototype sensors demonstrates these characteristics. A 0.47 m long liquid core fiber containing a liquid with a room temperature refractive index of 1.492 was analyzed. Both time- and intensity-domain behaviors around the device's critical temperature (95 °C) confirm theoretical expectations. Simultaneous strain and temperature measurements were performed between 95 °C and 105 °C. Methods for multiplexing liquid core fibers for increasing the range of temperatures that can be monitored were also investigated as well as using those liquid core fibers for cooling purposes.

Acknowledgments

I would like to express my appreciation to my advisor, Dr. Richard O. Claus for his guidance and ability to motivate me. I wish to thank Dr. K.A. Murphy and Dr. T.C. Poon for their comments, suggestions and for being on my advisory committee. I would also like to thank Dr. Ashish Vengsarkar and Bernd Zimmerman for their patience, encouragement and help on this project. The help and support I received from all the members in the Fiber & Electro-Optics Research Center, have made my work at the center very enjoyable over the past several years.

Finally I would like to thank my family and parents, Koop and Gerda de Vries, for their love, understanding and financial & moral support.

Table of Contents

List of Figures

1.0 Introduction

Fiber optic sensors have been an area of interest for researchers for more than a decade and several specific sensors for the measurement of strain, temperature, electric current, pressure and vibration have been developed [1]. The basic idea of modulating some property of the light propagating through an optical fiber has been exploited in several different ways; the principle of operation of a specific sensor depends on the modulation method being used. The most sensitive methods have incorporated the modulation of the phase of light propagating through the fiber and interfering the sensing beam with an unaffected reference beam to give rise to constructive and destructive interference patterns. Their implementation, however, requires complex stabilization methods, and this additional process often makes such sensors unattractive to commercial users whose requirements may not be very stringent. Intensity-based fiber optic sensors that are less sensitive than their phase-modulated counterparts are showing promise due to the inherent advantages of fiber optic sensing methods over conventional electrical techniques, namely, immunity from electromagnetic interference, small size, geometric flexibility and the possibility of using these sensors in harsh environments.

Liquid-core fibers were first investigated in 1972 as possible replacements for solid–core silica fibers which showed high transmission losses [2,3,4,5]. As the transmission losses through pure silica fibers were brought down, research in liquid-core fibers dwindled. In 1982, however, Kuribara and Takeda [6] used hollow-core fibers filled with Kerr-type liquids for voltage measurements and Hartog [7,8] followed with a distributed temperature measurement technique that used optical time domain reflectometry (OTDR) techniques to scan the backscatter from a liquid as a function of temperature. Huard and Viossat-Thomas used hollow core fibers filled with parrafins for monitoring the body

temperatures of patients during surgery [9]. Finally, in 1990, Soares and Dantas developed an intensity-type sensor based on the principle of the variation of the index of refraction of a liquid with temperature, by placing the core of a multimode fiber in a liquid with known index of refraction [10]

This thesis discusses how liquid core fibers can be used to measure both strain and temperature simultaneously. A theoretical analysis for measuring strain and temperature, by monitoring the time delay using an OTDR, is given and experimentally verified. An evanescentfield-based theory is used to describe the light output intensity changes with temperature and is also experimentally verified. The fabrication of liquid core fibers and of liquid core fiber interfaces, for temperature sensing, strain sensing and cooling are described in detail in this thesis. Methods for multiplexing liquid core fibers in parallel and in series as a means for increasing the range of temperatures that can be measured are also addressed.

2.0 Liquid Core Fiber (LCF) Sensor Fabrication

Liquid core fiber sensors maybe fabricated using a relatively inexpensive and uncomplicated process. The fiber sensor is manufactured using a hollow core silica fiber protected externally by either an acrylate or polyimide coating. Depending on the desired dimensional and index tolerances desired hollow core fibers can either be commercially obtained or custom manufactured. If tight tolerances are needed, the hollow core fiber can be drawn from a standard, undeposited silica fiber preform tube. Before the drawn hollow core fiber is filled, any air bubbles present in the fluid need to be removed. This is done by evacuating the air from the fluid using a vacuum pump or by pumping argon through the fluid. Pumping Argon through the fluid is a more efficient method since it removes air from the fluid while evacuation causes the fluid to evaporate as well. Once air bubbles are removed from the fluid the liquid core fiber is filled using the setup shown in Figure 2.1. A stopper with a hole in the center is plugged into the tube going to the
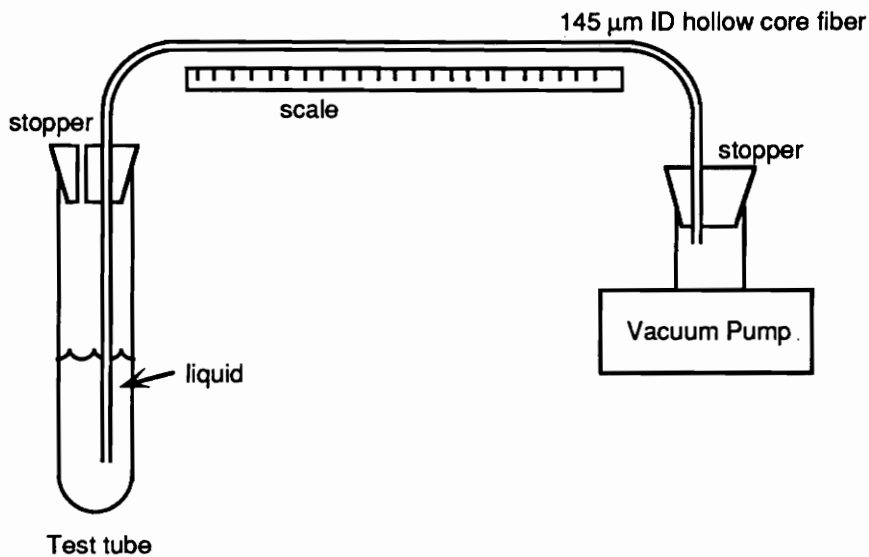
Figure 2.1 Setup used to fill the hollow core fiber.

vacuum pump. One end of the 145μm inner diameter hollow core fiber is threaded through the hole in the stopper and epoxied in place while the other end of the hollow core fiber is submersed in the fluid-filled test tube. Once the epoxy has cured the vacuum pump is turned on and the fiber is filled.

The coated hollow core fiber is filled with a fluid of desired optical properties by using a vacuum process. The fluids used range from optical grade, refractive index matching fluids [11] to industrial grade, high temperature silicone oils. The vacuum process itself can be accelerated by performing the fiber filling at elevated temperatures when fluid viscosities are lower than at room temperature. Figure 2.2 shows the results for filling the fibers at 19, 40, 58 and 75 °C, respectively, and shows that higher temperatures increase the filling rate [12]. This experiment was done using the setup shown in Figure 2.1, placed in a temperature controlled chamber. Multiple fibers can be filled at once in parallel with either the same fluid or with different fluids.

After the fiber has been filled, it can be cut to the required length, depending on the desired application. The liquid core fiber is accessed with standard silica core/clad fibers having an outer diameter ranging from 125 to 140 μm. The interfaces between the standard and the liquid core fibers are placed in capillary tubes filled with an index fluid which serve as fluid reservoirs, allowing free expansion and compression of the fluid within the liquid core fiber, (LCF) as temperature changes. These reservoirs have an outer diameter of approximately 2.0 mm, an inner diameter of 1.0 mm and measure 1.0 cm in length; the liquid core fiber reservoir and solid-core to liquid core interface is shown in Figure 2.3.
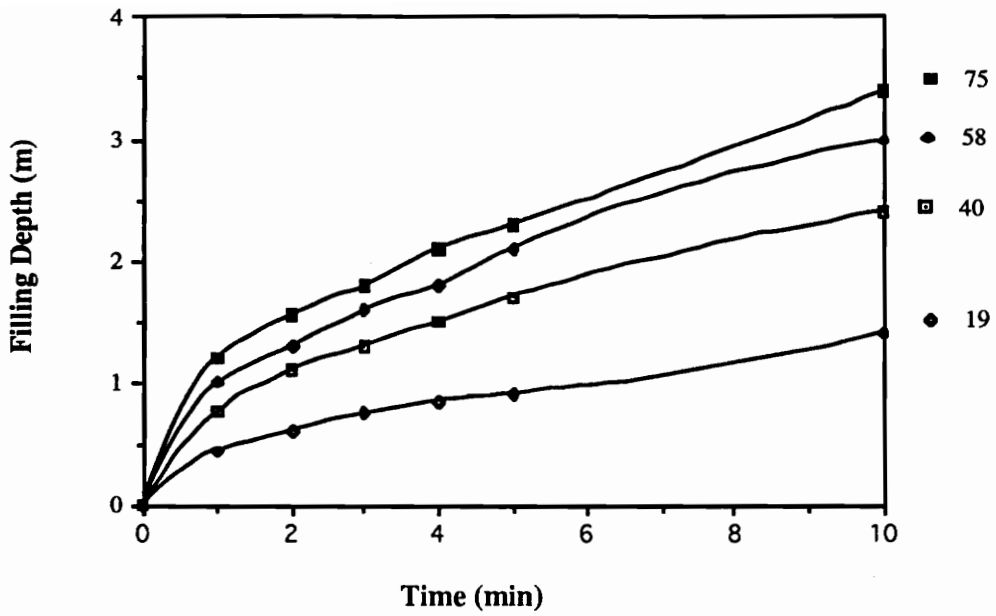
Figure 2.2. Hollow fiber filling at elevated temperatures.
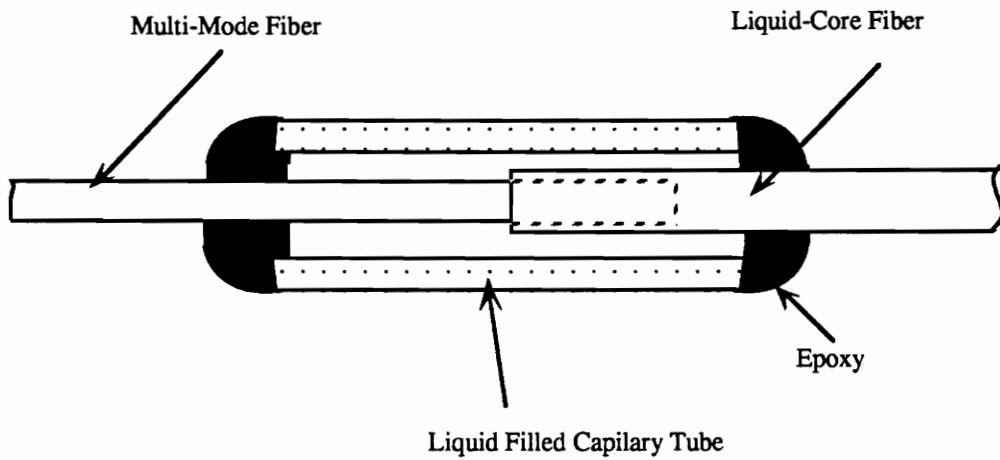
Figure 2.3. Liquid core fiber reservoir.

3.0 Optical Time Domain Reflectometry (OTDR) Review

An Optical Time Domain Reflectometer (OTDR) was used to demonstrate one possible approach for measuring temperature and strain using a liquid core fiber. The setup shown in figure 3.1 was used. It consists of a commercially available high resolution OTDR (which houses a pulsed laser diode which is repetitively triggered by a clock circuit, a detector, a delay generator, a sampler, and a signal processor), a display oscilloscope, and the liquid core fiber sensor [13,14,15].
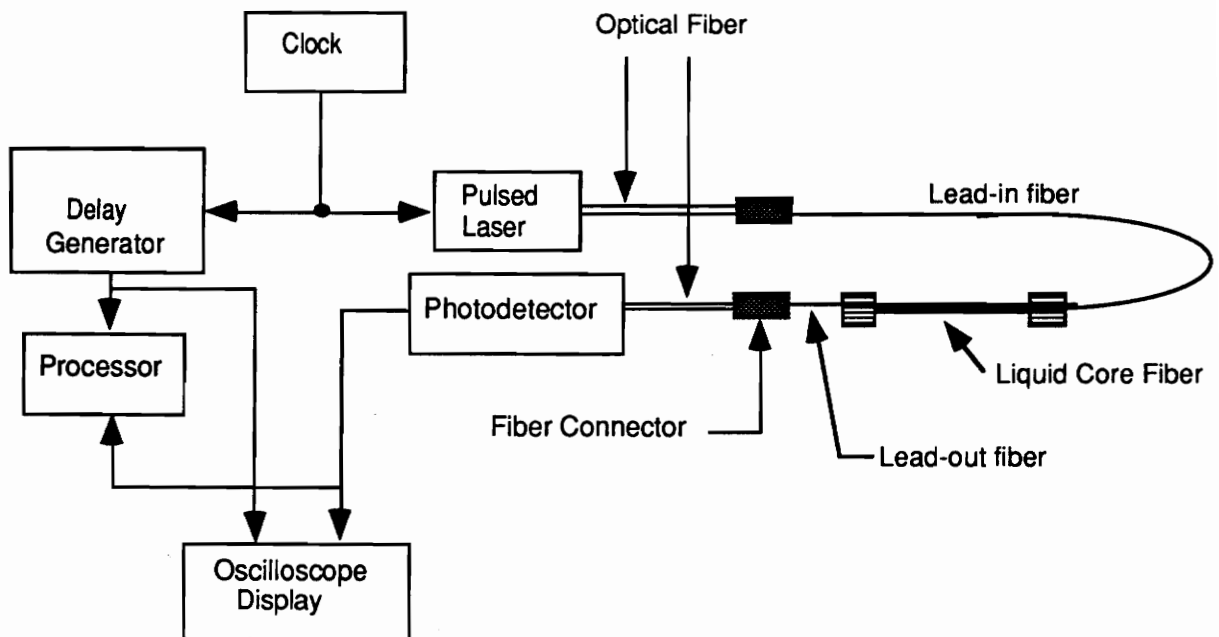
Figure 3.1. OTDR components

The OTDR measures the time of flight of a short optical pulse in an optical fiber, launched by a pulsed laser diode and detected by a detector. OTDRs are commonly used in the telecommunications industry to locate breaks in optical fiber cables. Knowing the speed of the light pulse in the fiber, it is possible to calculate the location of a break

(which reflects some of the pulse) by measuring the round trip time-of-flight of the light pulse to and from the break. The OTDR may be used for measuring strain in an optical fiber, since the strain induces a length change in the fiber and increases the time-of-flight of a pulse propagating through the fiber. In the case of the liquid core fiber the OTDR may also be used to measure temperature since the temperature changes the index of refraction of the core liquid and decreases the time-of-flight of the optical pulse. In our case, in order to eliminate pulse drifts, we monitor the pulse location with respect to a reference pulse that does not fluctuate in time. The reference pulse is generated by a reflection from the air gap in the connector joining the lead-in fiber to the pulsed laser pigtail fiber. This is done to reduce the effects of jitter in the pulsed laser repetition rate. The time resolution of the OTDR is approximately ± 2 ps, primarily due to laser jitter.

3.1 Strain Measurements using OTDR Techniques

In this section we discuss how strain measurements can be made using OTDR techniques. First, a detailed theoretical analysis is given concerning how a change in fiber elongation can be measured as a change in time-of-flight of an optical pulse. These theoretical results are then experimentally verified in the second section.

3.1.1 Theoretical Strain Measurement Analysis

When an axial strain is applied to an optical fiber the length of the optical fiber is changed. This change in fiber elongation can be determined using optical time domain methods where a change in the time-of-flight of an optical pulse that has traveled through the fiber can be measured. The time, t, required for an optical pulse to travel through an optical fiber of length, l, and refractive index, n, can be determined by

$$t = \frac{nl}{c}, \tag{3.1}$$

or by,

$$t = \frac{1}{v_g}, \tag{3.2}$$

where c is the speed of light in free space and v_g is the group velocity of the optical pulse. By differentiating both sides of equation (3.1) we obtain [15]

$$dl = \frac{cdt}{n} - \frac{tcdn}{n^2}. \tag{3.3}$$

Substituting equation (3.1) into equation (3.3) we now obtain

$$dl = \frac{cdt}{n} - \frac{ldn}{n}. \tag{3.4}$$

The axial strain, ε, on an optical fiber is expressed as elongation divided by the total length of the optical fiber. By examining equation (3.4), one observes that a change in the length of an optical fiber results in a change in the arrival time of the optical pulse as well as a change in the refractive index of the fiber. The change in index of refraction of the fiber is dependent on the axial strain applied to the fiber and can be determined from equation (3.5) below,

$$\frac{dn}{n} = a\varepsilon, \tag{3.5}$$

where the photo-elastic coefficient, a, of the optical fiber can be determined for each optical fiber by applying a strain to the fiber in a load frame. Once the photo-elastic coefficient has been determined equation (3.4) can be expressed as

$$\Delta l = \frac{c\Delta t}{n}\left(\frac{1}{1+a}\right), \tag{3.6}$$

Figure 3.2 gives a plot of the theoretical shift of an optical pulse caused by elongation of hollow core, solid core and liquid core optical fibers, with indices of 1.0, 1.45 and 1.492, respectively.
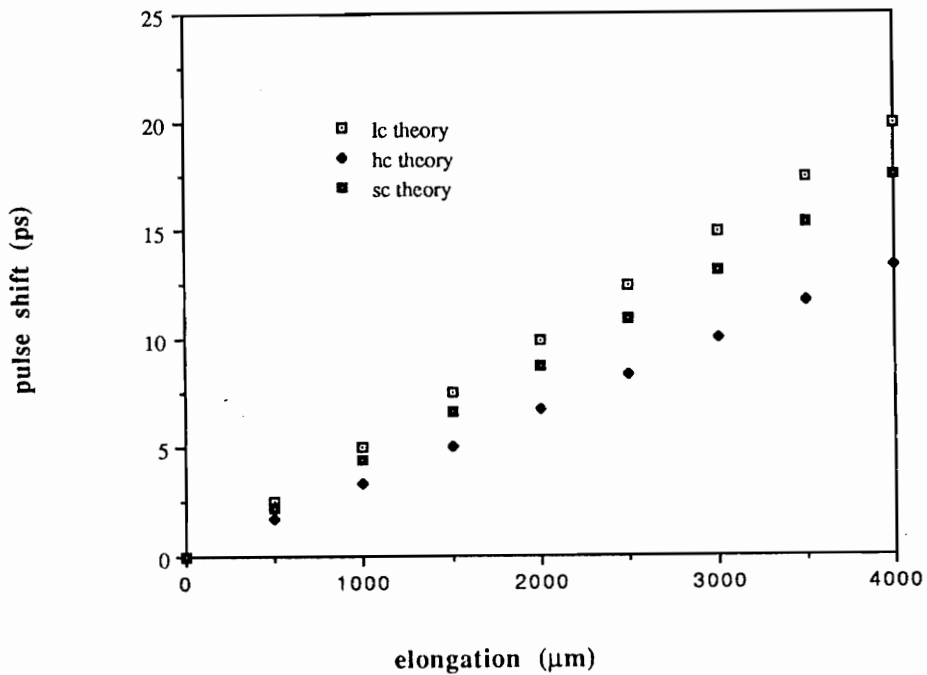
Figure 3.2 Theoretical pulse shift as a function of elongation for hollow core, solid core and liquid core optical fibers.

3.1.2 Experimental Verification

In order to verify equation (3.5), and the results shown in Figure 3.2, the change in time-of-flight of an optical pulse in a hollow core fiber, where n=1, a solid core fiber, where n=1.45 and a liquid core optical fiber where n=1.492, as a function of elongation, were determined using an optical time domain reflectometer. In the cases of the hollow core fiber and the liquid core fiber, no photoelastic coefficient is present. The hollow core, solid core and liquid core fibers were strained by attaching the fibers to posts and translating one post, as shown in Figure 3.3, with a micropositioner. This experiment demonstrates the feasibility of measuring strain with the optical fibers.
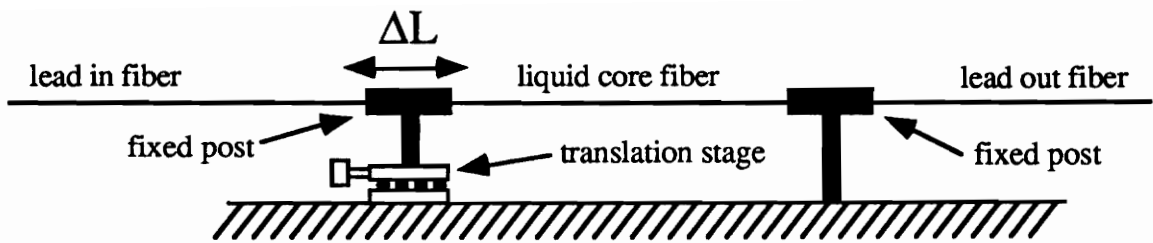
Figure 3.3. Setup used for measuring strain.

The plotted results of this experiment, in Figure 3.4, show that an increase in elongation results in an increase in pulse shift. The results in Figure 3.4 also show that the liquid core fiber is most sensitive to elongation. This is due to the fact that the liquid core fiber has a higher index of refraction than either the hollow core fiber and the solid core fiber. By choosing a liquid core fiber with an even higher index of refraction, (indices up to 2.0 are available), even more sensitivity can be obtained. For example, once optical losses in sapphire fibers are reduced, sapphire fibers could also be used for making strain measurements that are more sensitive to strain than silica optical fibers.
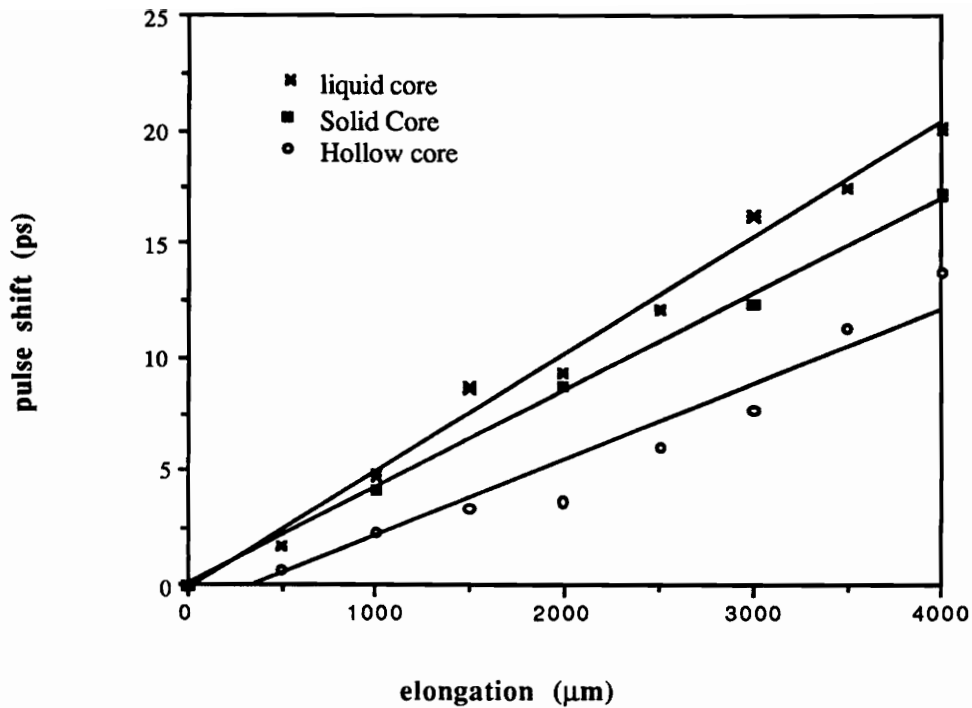
Figure 3.4. Elongation versus pulse shift for hollow core, solid core and liquid core optical fibers.

3.2 Temperature Measurements using OTDR Techniques

This section demonstrates that OTDR techniques can be used to measure temperature in liquid core fibers. A detailed theoretical analysis shows how a change in temperature results in a change in time-of-flight of an optical pulse. The results are then experimentally verified.

3.2.1 Theoretical Temperature Measurement Consideration

In order to accurately measure strain it is important to be able to predict the effects of temperature as well and to compensate for cross-sensitivity. In equation (3.4), the change in time of flight can be accurately determined, with a resolution of 2 ps or better, and an accurate value for the index of refraction of the core fiber can be obtained from the manufacturer. By solving equation (3.4) for change in time of flight we obtain

$$dt = \frac{ndl}{c} + \frac{ldn}{c}. \tag{3.7}$$

The changes in time delay with respect to a change in temperature can then be expressed as

$$\frac{dt}{dT} = \frac{n}{c}\frac{dl}{dT} + \frac{l}{c}\frac{dn}{dT}, \tag{3.8}$$

where

$$\frac{dl}{dT} = \alpha l, \tag{3.9}$$

and where α is the effective coefficient of thermal expansion of the fiber (which for a silica fiber is on the order $7 \times 10^{-7}/^{\circ}C$) [16]. Changes in index of refraction as a function of temperature can be expressed as

$$\frac{dn}{dT} = \beta n, \tag{3.10}$$

where the change of n with respect to temperature is on the order of 2×10^{-5} for a glass fiber and 4×10^{-4} for a liquid core fiber. Using equations (3.9) and (3.10) from above in equation (3.8) we obtain

$$\frac{dt}{dT} = \frac{n}{c}\alpha l + \frac{1}{c}\beta n. \tag{3.11}$$

Since the index change as a function of temperature contributes more to the time delay than the change in length as a function of temperature, the coefficient of thermal expansion for an optical fiber can be omitted, leaving us

$$\frac{dt}{dT} = \frac{1}{c}\beta n. \tag{3.12}$$

In the case of a solid core fiber the change in time of flight as a function of temperature is 20 times smaller than the change in time of flight for a liquid core fiber. The pulse shift for a solid core fiber as a function of temperature is 0.07ps/°C whereas for a liquid core fiber the pulse shift is 1.3ps/°C (assuming a fiber length of one meter).

3.2.2 Experimental OTDR Temperature Measurements

To verify the possibility of using a liquid core fiber as a temperature sensor the experimental setup shown in Figure 3.5 was used. The fiber was placed in a metal tube that was filled with a high temperature silicone oil, such that a uniform temperature could be applied to the fiber. Stoppers with tiny holes were placed on the ends of the metal tube such that strain could also be simultaneously exerted. Heating tape was wrapped around the pipe and insulating tape was wrapped around the heating tape to ensure good insulation.

Figure 3.5. Setup used for measuring temperature.

The temperature of the oil bath was slowly increased and monitored with a thermocouple, while the time delay of an optical pulse relative to a reference pulse was also monitored, using an OTDR, as shown in Figure 3.1. The time-of-flight of a pulse in this fiber changes, due to the change in refractive index (and consequently, the speed of light in the silicone oil) induced by the change in temperature (the thermooptic effect). The results, plotted in Figure 3.6 show that an increase in the temperature of the oil bath corresponds to a negative pulse shift. The negative pulse shift is caused by the negative thermooptic coefficient of the fluid in the liquid core fiber.
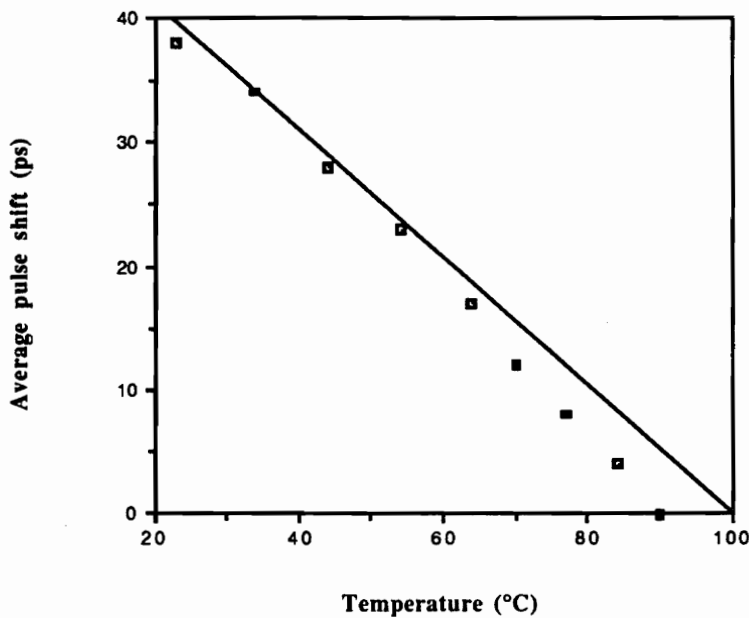
Figure 3.6. Temperature versus average pulse shift

4.0 Evanescent Based Temperature Sensor

A model for an evanescence-based liquid fiber sensor is developed based on weakly-guiding theory and an experiment demonstrates that the results closely approximate the theoretical model.

4.1 Evanescent Field Theory

In this section, we derive a simple model for the evanescence-based liquid fiber sensor. The model, based on weakly-guiding theory, assumes no dependence on the length of the sensor fiber. We will see that despite the simplifying assumptions, we obtain a fairly accurate model that matches the experimental results.

From the weakly-guiding theory, the ratio of the power in the clad to the total power in the fiber for a specific mode n is given by [17]

$$\left(\frac{P_{clad}}{P_{total}}\right)_v = \frac{U^2}{V^2}(V^2-U^2)^{\frac{1}{2}},$$

(4.1)

where $U^2 = k_0^2\, a^2\, (n_1 2 - \beta v^2)$, $V^2 = k_0^2\, a^2\, 2\, (n_1^2 - n_2^2)$, βv is the propagation constant of the mode, a is the core radius, and n_1 and n_2 are the refractive indices of the core and the cladding, respectively. In Equation (4.1), V is a normalized frequency parameter of the fiber and $k_0 = 2\pi/\lambda$, where λ is the free space wavelength of operation. U stays between successive roots of the Bessel functions, the values of which are very close to each other. In fact, we can show that $U_\infty - U_c \approx \pi$, where U_∞ is the far-from-cutoff value of U and U_c is the cutoff value. Hence, we can replace U in Equation (4.1) by U_c. We can also show that a good approximation to U_c is given by $U_c = (2v)1/2$, where n is the order of the

mode. Since N, the total number of modes in a weakly-guiding fiber, is given by $V^2/2$, Equation (4.1) can be rewritten as

$$\left(\frac{P_{clad}}{P_{total}}\right)_v = \frac{v}{N}(2N-2v)^{-1/2}. \tag{4.2}$$

The average ratio for all the modes $v = 1, 2, \ldots N$, can then be found by integrating over all v's and dividing the result by the total number of modes N. This gives

$$\left(\frac{P_{clad}}{P_{total}}\right)_{avarage} = \frac{1}{N}\int_0^N \frac{v}{N\sqrt{2}\sqrt{N-v}}\,dv = \frac{2\sqrt{2}}{3\sqrt{N}}. \tag{4.3}$$

Since $P_{core} + P_{clad} = P_{total}$, and V contains the variable n_1, which changes in the sensor, the ratio (P_{core}/P_{total}) is a function of n_1. For a liquid with a linear refractive index dependence on temperature one can plot the variation of the ratio (P_{core}/P_{total}) as a function of temperature as shown in Figure 4.2. For comparison, we have also shown one of the experimental plots. Note that although the units on the two y-axes are not of the same order, the behavior of the sensor is predicted appropriately by the theoretical model.

4.2 Experimental Verification

The basic intensity based liquid core fiber set-up is shown in Figure 4.1. It consists of an optical source such as a HeNe gas laser, the liquid core fiber sensor (including lead fibers), and a photodetector. The output of the laser is launched into the lead fiber of the sensor using a collimating lens and a fiber holder. The output of the sensor is directed through the lead fiber directly onto the photodetector without the use of collimating

lenses. The output of the detector is then amplified and displayed by a commercially available optometer. The temperature surrounding the LCF is applied through a heated bath of high temperature silicone oil such that uniform temperature changes are insured.
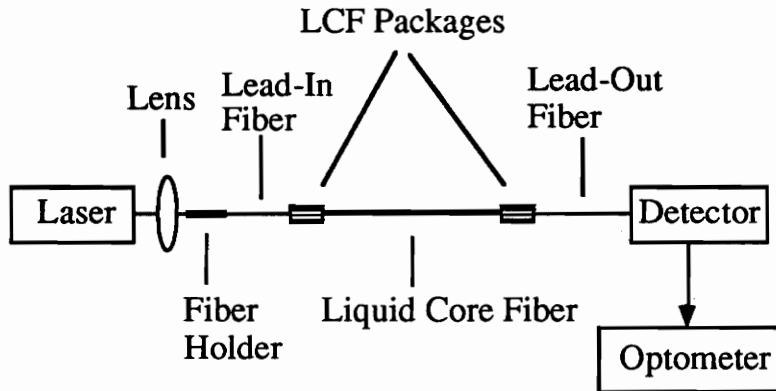
Figure 4.1. Transmissive, intensity-based liquid core fiber temperature sensor setup.

This setup was used to characterize the performance of LCF sensors with various fluids. The change in index with respect to temperature for all tested fluids was approximately -4.0×10^{-4} /°C. The results of this experiment are shown in Figure 4.2. By choosing liquids with different indices of refraction different regions of sensitivity can be obtained. In the next section we demonstrate how one can use multiplexing techniques to increase the range of temperatures that can be monitored using liquid core fibers.

LCF: Theory vs. Experiment
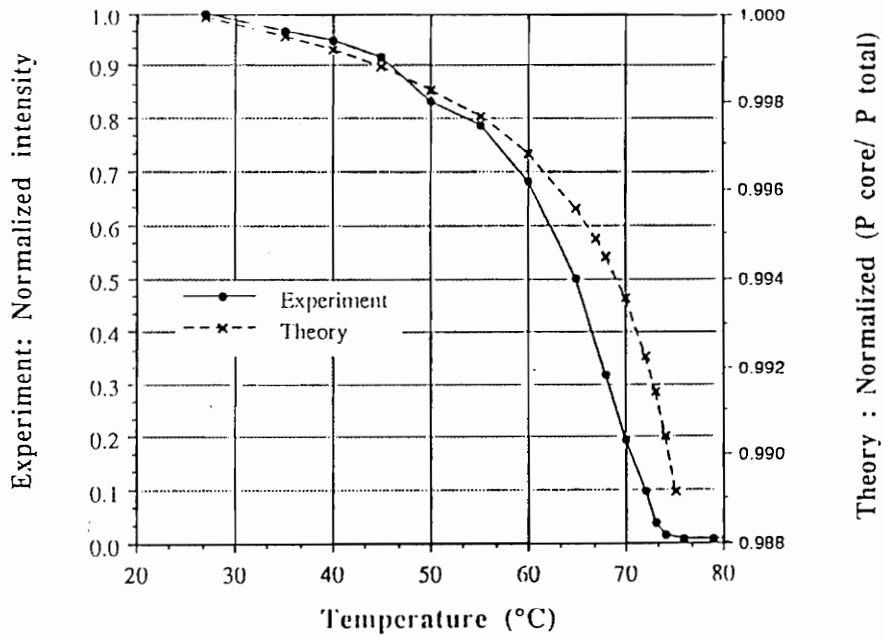
Figure 4.2. Comparison of experimental and theoretical results.

5.0 Liquid Core Fiber Multiplexing Methods for Temperature Sensing

One of the drawbacks of using liquid core fiber sensors is the limited temperature range in which each sensor is effective. In order to demonstrate that liquid core fiber sensors can be used to perform measurements over a wider range of temperatures, two different multiplexing techniques were investigated. For the first method a parallel multiplexing scheme was developed that allowed for temperature measurement from 25 to 185 °C. The second method investigates the in-line multiplexing capabilities of the sensors by using a high resolution OTDR in the reflective mode and placing liquid core fiber sensors separated by semi-reflective splices in series.

5.1 Parallel Multiplexing

By choosing liquids with different indices of refraction different regions of sensitivity can be obtained [18, 19]. From Figure 5.1, one observes how eight liquids with different regions of sensitivity can be combined to cover temperatures form 25 °C to 185°C. Placing these different sensors in parallel, as shown in Figure 5.2, allows for monitoring a wider range of temperatures. The maximum number of sensors that can be multiplexed in series depends entirely on the insertion and excess losses in the coupler. For practical applications a switch may be needed to address each individual sensor. The results from Figure 5.1 demonstrates that different liquids suitable for different temperature ranges are commercially available.

Figure 5.1. Parallel multiplexing of several fiber sensors for increased temperature range.

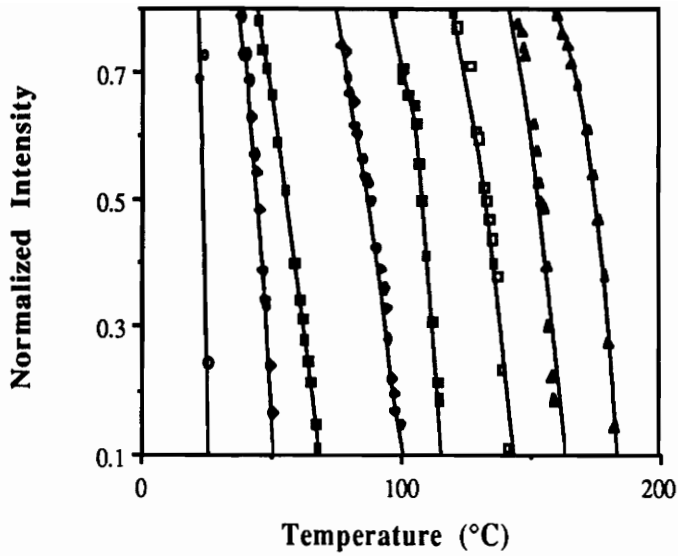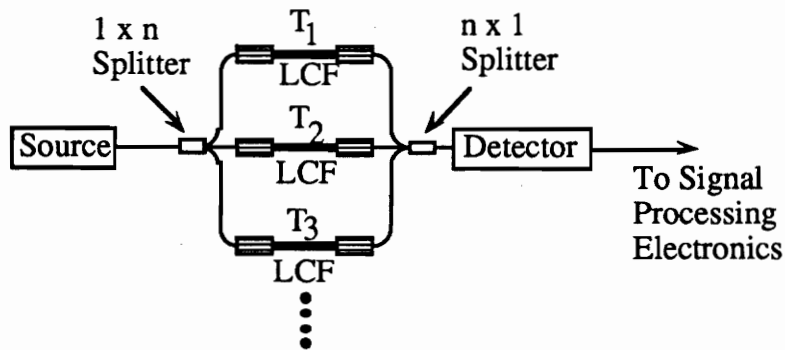

Figure 5.2 Setup for placing liquid core fibers in parallel.

5.2 Multiplexing in Series

To demonstrate in-line multiplexing capabilities of liquid core fiber sensors the set up shown in Figure 5.3 was implemented. The setup consisted of the high resolution OTDR,

setup as described in section 3 (this time the OTDR operates in the reflective mode while the OTDR in section 3 operated in the transmissive mode) and the in-line liquid core fiber sensors. The in-line sensors consisted of two liquid core fibers with room temperature fluid refractive indices of 1.512 and 1.492 separated from each other by a lead fiber containing a partially reflective splice.
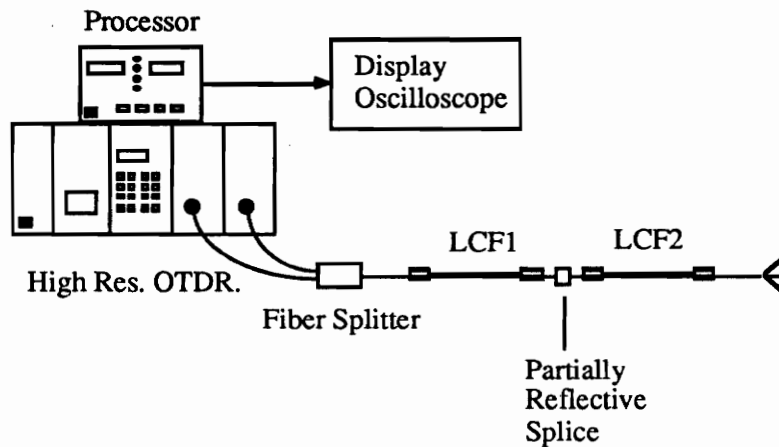
Figure 5.3 Reflective, intensity-based liquid core fiber temperature setup.

The sensor with the higher room temperature refractive index fluid was placed closest to the laser/detector, such that propagation through LCF1 was ensured beyond the cutoff temperature of LCF2 when the fiber of LCF2 stops propagating light. Both sensors were immersed in a silicone oil bath and monitored while temperature was slowly increased. Between 70 °C and 95 °C the reflected pulse intensity from the lead out fiber of the far end LCF sensor was monitored while the reflection of the partially reflective splice between the two sensors was monitored from 95 °C to 125 °C. This technique allows continuous temperature monitoring between 70 °C and 125 °C. Figure 5.4 shows the results obtained by placing the two liquid core fibers in series. The filled circles represent data points from LCF2 while crosses represent LCF1 data.
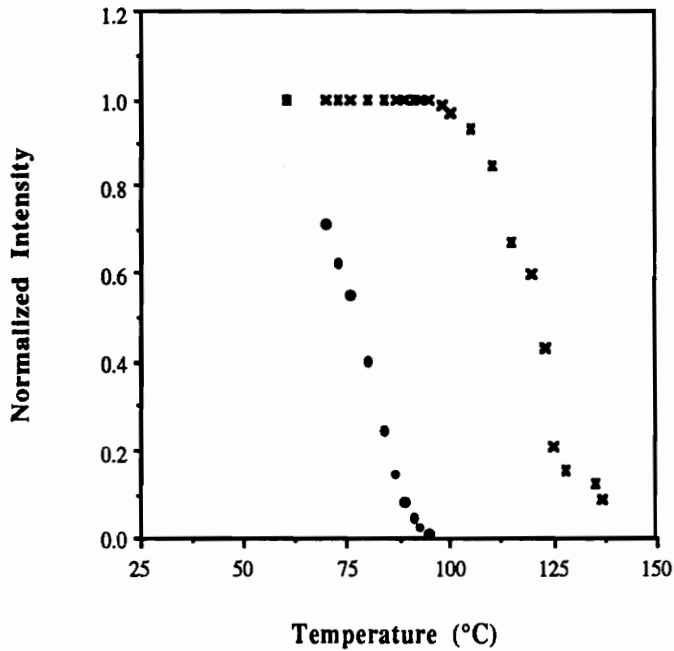
Figure 5.4. Variation of normalized transmitted intensity as a function of temperature for two sensors in series.

The limitations on the maximum number of sensors that can be multiplexed using this multiplexing method are dependent on the dynamic range of the OTDR, the signal-to-noise ratio and the pulse dispersion introduced by the liquid core fiber. Figure 5.5 shows a setup that could be used for multiplexing more than two sensors in series.
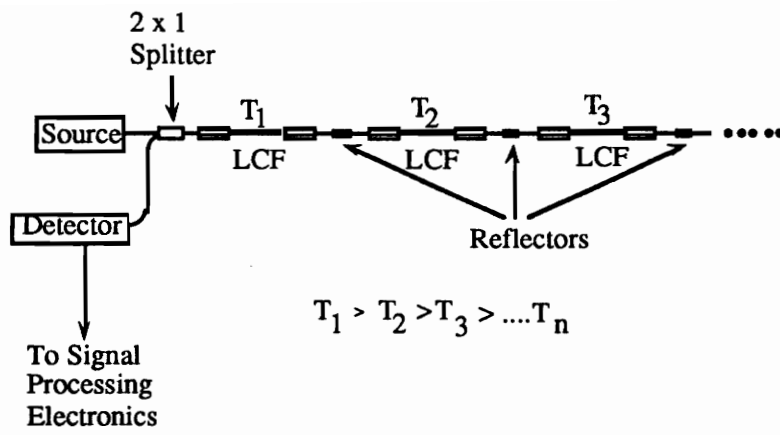
Figure 5.5. Series multiplexing of several fiber sensors for increased temperature range.

6.0 Simultaneous Measurement of Strain and Temperature

In order to demonstrate that a single piece of fiber can be used as a dual parameter sensor for simultaneous strain and temperature measurements we show that changes in transmitted signal intensity and time-of-flight of an optical pulse allow for simultaneous monitoring of strain and temperature.   In the experiment to verify this dual parameter sensor we used a liquid core optical fiber consisting of a hydrogenated terphenyl core and a polyimide coated silica cladding. The liquid core was chosen to have an index of refraction, $n_c(T_0, E_0)$ of 1.492 resulting in a step-index fiber.   An optical signal launched into the fiber will propagate with relatively low signal attenuation. However, signal attenuation increases as temperature and or strain are applied to the fiber such that the difference between core and cladding refractive indices diminishes. Once the core refractive index exceeds that of the cladding, the signal is no longer confined to the core, and significant power losses can be observed. This condition can be achieved by either increasing the temperature surrounding the fiber until the core refractive index drops below that of the silica cladding or straining the fiber until the cladding refractive index falls above that of the liquid core. The equation governing this condition where core and cladding refractive indexes are approximately equal is given by:

$$n_c(T_0,\varepsilon_0)(1 + \beta\Delta T) = n_{cl}(T_0,\varepsilon_0)(1 + \alpha_{cl}\varepsilon), \tag{6.0}$$

where β_c is the thermo-optic coefficient of the liquid, T is the temperature surrounding the fiber, T_0 is the room-temperature, α_{cl} is the photo-elastic coefficient of the cladding, ε_0 is an arbitrary fiber control strain, and ε is the actual strain applied to the fiber. It is assumed that the photo-elastic coefficient of the fluid, as well as the thermo-optic coefficient of the cladding are negligible in this analysis.

A 0.47 m long liquid core fiber with an inner diameter of approximately 150 μm and a room temperature refractive index of 1.492 was fabricated. The fiber was contained in a chamber of silicone oil, as shown in Figure 3.5, for uniform temperature application such that axial strain could also be simultaneously exerted, as shown in Figure 3.2. In the actual setup the setups are combined into one, such that the liquid core fiber could be strained and heated simultaneously . The fiber output was monitored using a picosecond resolution, wide dynamic range optical time domain system described in section 3. The reference signal which was periodically updated, was tapped off from the lead-in fiber to compensate for both time and intensity-drift of the laser. The 850 nm laser which emits a 220 ps wide pulse, was triggered at 30 kHz. The monitoring system and chamber thermocouple were interfaced with an IBM personal computer through a GPIB bus and an A/D board. Acquired data which included temperature, strain, time-of-flight, pulse width (FWHM), and transmitted intensity, were stored on the computer and analyzed after the completion of the experiments.

The change in time-of flight of a pulse is influenced by both the elongation of the fiber and the change in temperature of the fiber. While the output intensity of the optical fiber is also dependent on the fiber elongation and change in fiber temperature. The following linear system of equations needs to be evaluated.

$$\Delta\tau = A\Delta L + B\Delta T, \tag{6.1a}$$

$$I = C\Delta L + D\Delta T, \tag{6.1b}$$

where $\Delta\tau$ is the compensated change in pulse time-of-flight and I represents P_{sig}/P_{ref} in arbitrary units. The change in fiber length, ΔL, and the change in temperature, ΔT, demonstrate the cross sensitivity of the two equations. To resolve the temperature and strain in the sensing system the four constants, A, B, C, D must be determined. Four

experiments were conducted in order to obtain each of the coefficients. Strain and temperature can only be monitored in a limited temperature region for liquid core fibers. For the fiber chosen in this experiment the region where strain and temperature can be simultaneously monitored lies between 95 °C and 106 °C. Figure 6.2 shows how pulse intensity, time-of-flight and pulse width (FWHM) of an optical pulse change with temperature and only in the region where the pulse intensity changes due to strain or temperature are simultaneous measurements of strain and temperature possible.

6.1 Measurement of Intensity as a Function of Temperature

To obtain the liquid core fiber temperature constant D in Eq. (6.1b), the fiber was heated while no strain was applied to the fiber. Equation 6.1b then becomes

$$I = D\Delta T. \tag{6.2}$$

Constant D was determined by measuring the intensity of the optical pulse injected into the fiber by the OTDR. The experimental setup described in the previous section was used. To insure uniform heating the silicone oil was slowly heated and the intensity of the optical pulse was monitored as a function of temperature. Figure 6.1 shows how the pulse intensity slowly starts to decrease once the temperature exceeds 80 °C, sharply drops above 95 °C and is reduced to nearly zero at 106 °C. The temperature drop from 95 °C to 106 °C is considered to be the sensing region of the sensor since in this region the sensor is most sensitive to changes in temperature and the drop off in intensity is almost linear. By looking at the linear region of this graph the D coefficient is determined to be 2.5/°C.
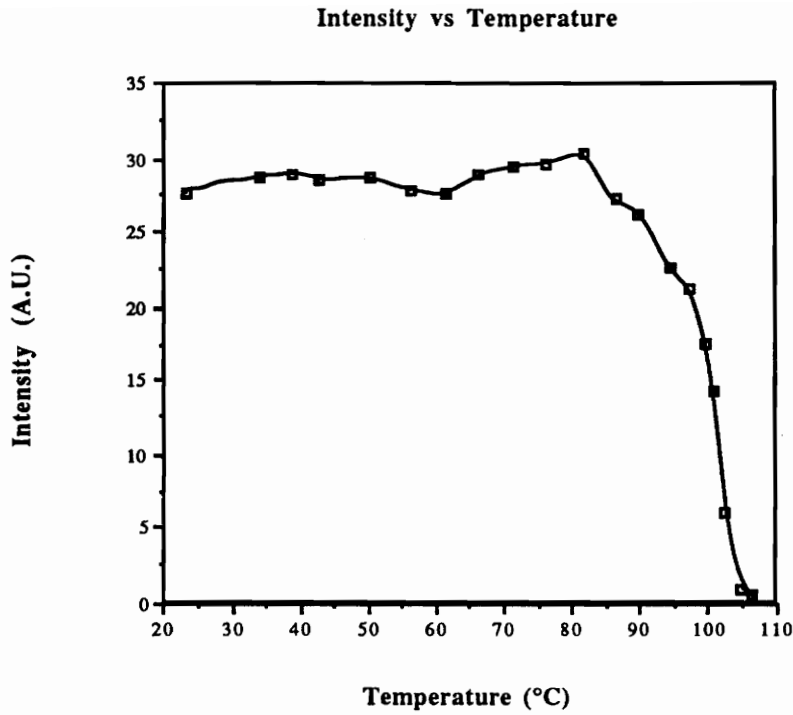
Intensity vs Temperature

Figure 6.1. Liquid core fiber sensor temperature response (Intensity) with zero strain.
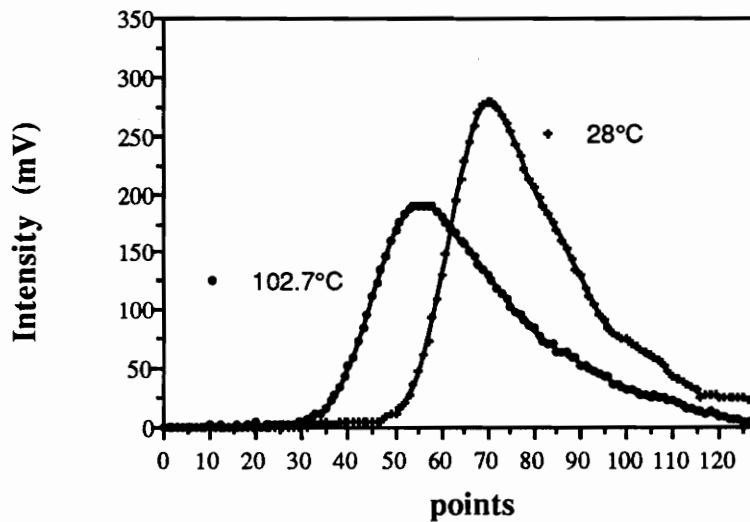
Figure 6.2. Liquid core fiber sensor response to temperature, i.e. changein FWHM,

Intensity and time-of-flight of an optical pulse.

6.2 Measurement of Intensity as a Function of Strain

To determine coefficient C in equation (6.1b) the fiber was axially strained at different constant temperatures, i.e. $\Delta T=0$. Equation 6.1b is reduced to,

$$I = C\Delta L. \tag{6.3}$$

In this experiment the fiber is axially strained while the temperature surrounding the fiber was held constant. The output intensity of the optical pulse was monitored using the OTDR system, while the fiber was axially strained at room temperature, 80 °C and 102.4 °C. The results are shown in Figure 6.3. At both room temperature and 80 °C the intensity did not change with elongation. While at 102.4 °C and zero strain, when the intensity has dropped considerably, the output intensity does increase when the strain on the liquid core fiber is increased. This is caused by a decrease in the index of refraction of the cladding due to an increase in strain thereby making the liquid core fiber a waveguide. From Figure 6.3 a value of 2.56/mm can be obtained for the C coefficient in equation 6.3.
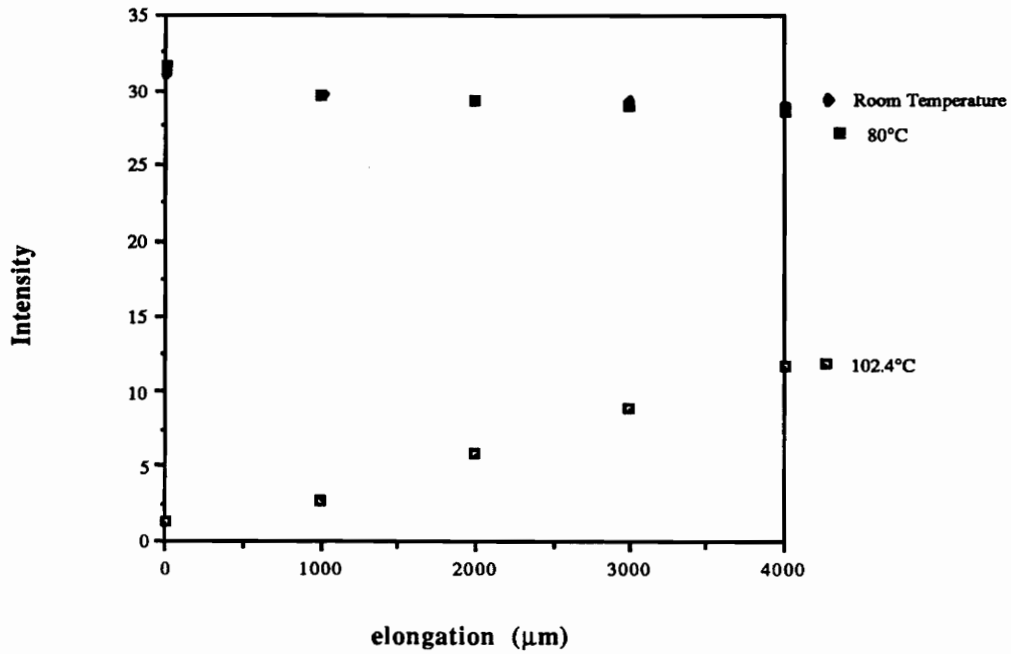
Figure 6.3. Intensity as a function of elongation at room temperature, 80 °C and 102.4 °C.

6.3 OTDR Strain measurement

Strain constant A, in equation 6.1a, was obtained by straining the liquid core fiber while keeping the temperature surrounding the liquid core fiber constant, ie. $\Delta T=0$. Equation 6.0a then becomes

$$\Delta \tau = A\Delta L. \qquad (6.4)$$

By elongating the fiber and monitoring both the time delay and the change in the full width half maximum (FWHM) of the optical pulse, constant A was determined using the experimental setup described before. The fiber was first elongated and the change in time-of-flight was monitored at room temperature, 80 °C and 102.4 °C, as shown in figure 6.4. At room temperature and at 80 °C, when the fiber was strained, a change in

the time-of-flight of the optical pulse was observed, just as expected. At 102.4 °C the change in time delay of the optical pulse with elongation was minimal. The change in pulse width, or full width half maximum (FWHM), was also observed at room temperature, 80 °C and 102.4 °C as shown in Figure 6.5. At room temperature and 80 °C the optical pulse FWHM did not change much, while at 102.4 °C the FWHM of the optical pulse decreased as the fiber was elongated. The change in pulse width of the optical pulse and minimal change in time delay of the optical pulse, after the critical temperature was reached, can be explained by analyzing Figure 6.2. In Figure 6.2 the FWHM of the optical pulse increases as the intensity of the pulse decreases. As a consequence of this change in pulse shape, the change in FWHM and intensity of the optical pulse also changes the location of the optical pulse peak, which is used to determine the time delay of the pulse. As it turns out when change in FWHM is subtracted from change in time delay as a function of elongation, the expected result is obtained as shown in Figure 6.6. From Figure 6.6 a value of 4.4ps/mm is obtained for coefficient A.
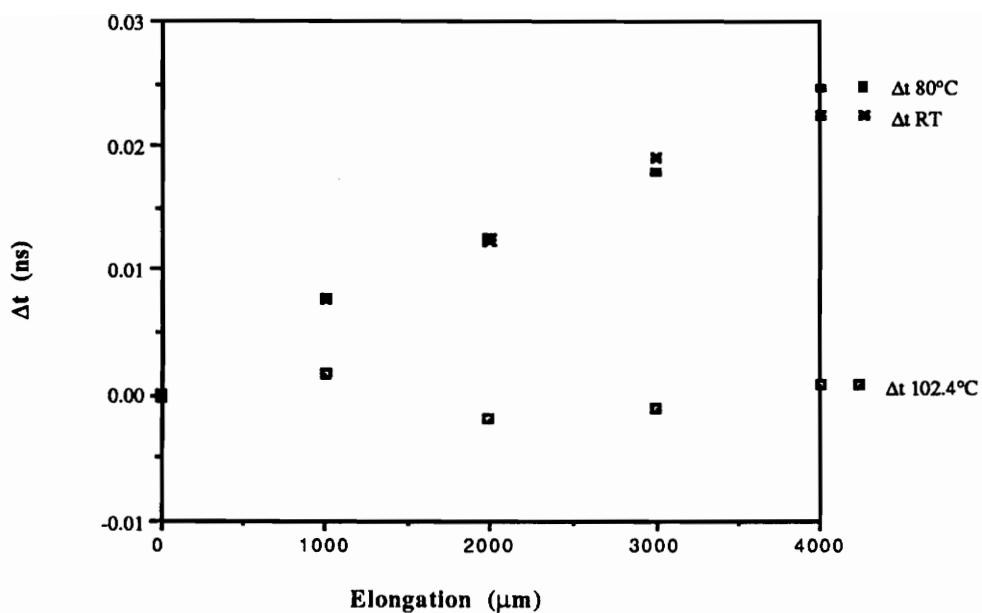
Figure 6.4 Optical time delay as a function of elongation at room temperature, 80 °C and
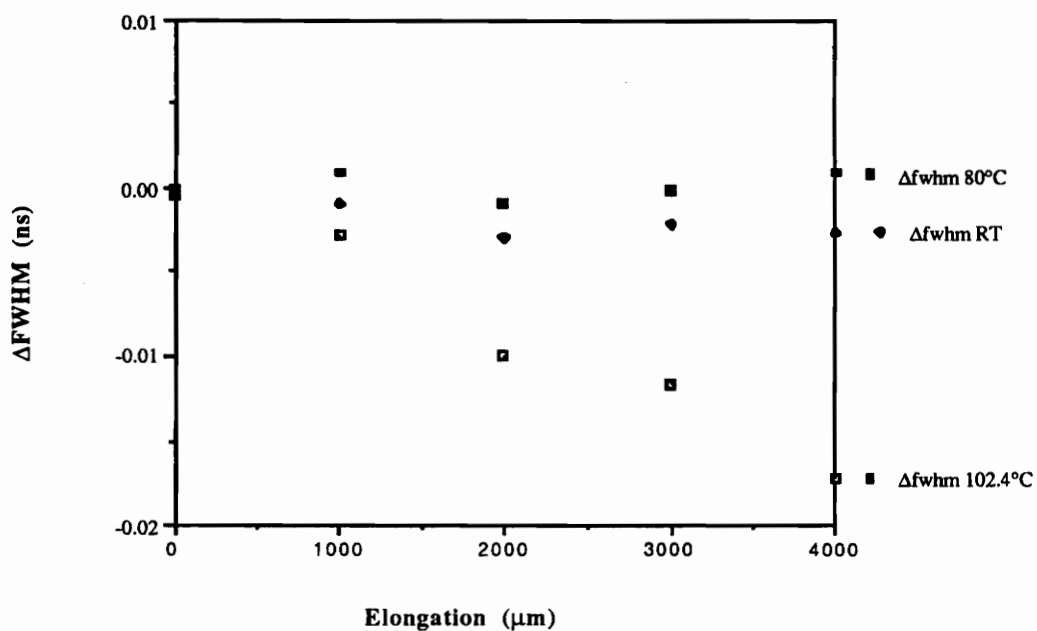
102.4 °C.

Figure 6.5. Change in FWHM as a function of elongation at room temperature, 80 °C
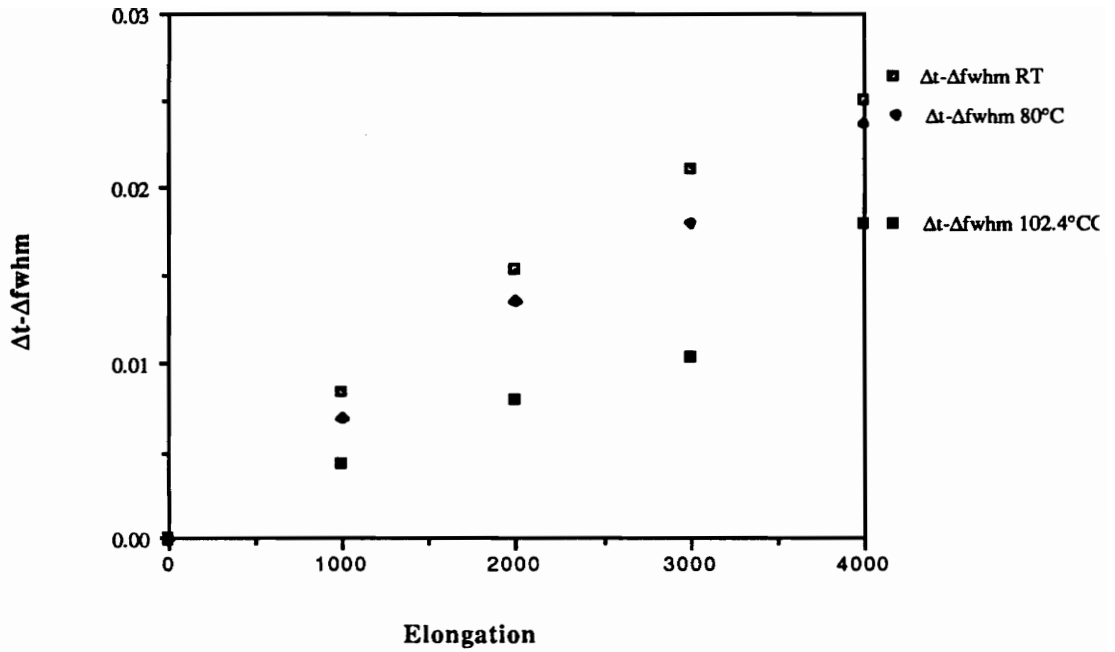
and 102.4 °C.

Figure 6.6 Change in FWHM subtracted from change in time delay at room temperature, 80 °C and 102.4 °C.

6.4 OTDR Temperature measurement

Finally to determine temperature coefficient B in equation 6.1a the liquid core fiber sensor was heated at zero strain ($\Delta L=0$). Therefore equation 6.1a becomes

$$\Delta\tau = B\Delta T. \tag{6.5}$$

By monitoring the change in time of flight of the optical pulse as the temperature is slowly increased, temperature coefficient B is determined. The setup described in the introduction of section 6 was used. Figure 6.7 demonstrates that as the temperature

increases the change in time delay of the pulse decreases until the critical temperature is reached, at which point the change in optical time delay increases. Figure 6.8 demonstrates that the FWHM does not increase with temperature until a critical temperature is reached, at which point the change in FWHM increases. A similar effect has been observed in the previous section. As the temperature increases, the intensity of the pulse decreases and the optical pulse FWHM increases. This change in pulse intensity, and FWHM also changes the location of the pulse peak and consequently changes the time delay with temperature. Again, as it turns out when the change in FWHM is subtracted from the change in optical time delay the desired result is shown in Figure 6.9, is obtained. From this graph coefficient B can be obtained to be 0.9ps/°C.

Figure 6.7. Optical time delay as a function of temperature.
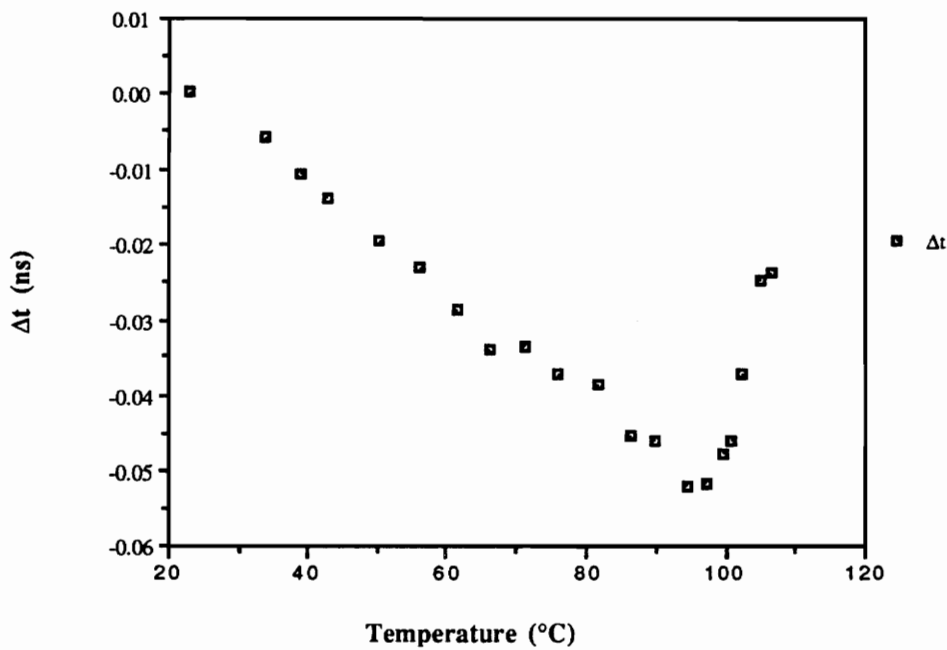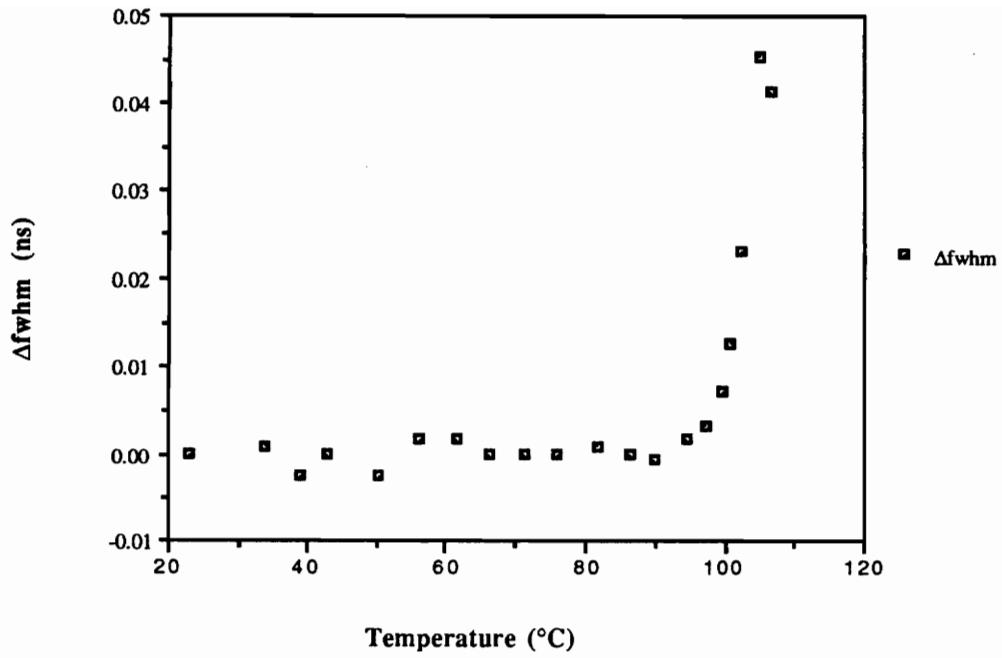
Figure 6.8 Optical FWHM as a function of temperature.
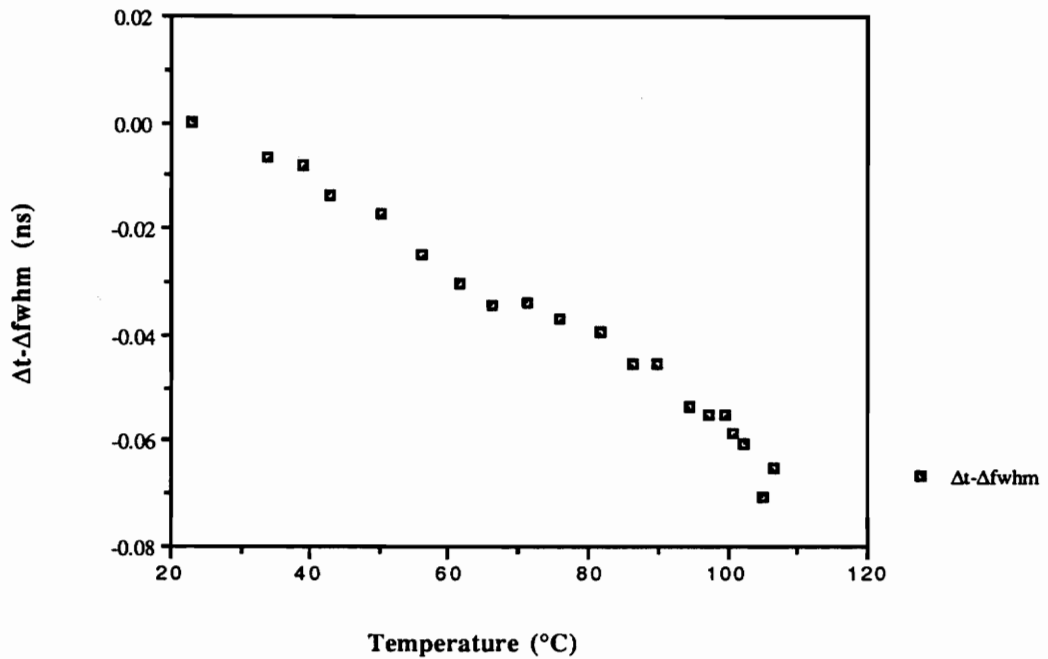
Figure 6.9 Change in FWHM subtracted from change in time delay as a function of

temperature.

To summarize the experimental results the coefficients A, B, C and D are listed below.

A = 4.4ps/mm

B = 0.9ps/°C

C = 2.56/mm

D = 2.5/°C

6.5 Resolution of the Sensing System

In order to determine if a small change in the $\Delta\tau$ or I in equations 6.1a or 6.1b leads to a large change in the solution, the condition number of this equation is determined [20,21].

$$\Delta\tau = A\Delta L + B\Delta T, \tag{6.1a}$$

$$I = C\Delta L + D\Delta T. \tag{6.1b}$$

The condition number of a matrix gives an indication of how well the matrix is conditioned, and is always greater than one. When the condition number is very large the solution of the equation Ax=b will be very sensitive to relatively small changes in b, while if the condition number is close to 1 the solution of Ax=b will not be sensitive to small changes in b. A system with a small condition number is called well-conditioned while a system with a large condition number is considered to be ill-conditioned.

In order to calculate the condition number of matrix A the norm of matrix A and A^{-1} must be calculated using the relation below.

$$\|A\| = \max_{1 \le i \le n} \sum_{j=1}^{n} |a_{ij}|, \tag{6.5}$$

The condition number can then be obtained using

$$\text{Cond}(A) = ||A|| \, ||A^{-1}|| \, . \quad (6.6)$$

Since the condition number of a matrix is always greater than one the reciprocal of the condition number rcond(A) has to lie between zero and one. In previous Analyses by Wang et al a rcond(A) was obtained of 0.001, while Vengsarkar et al calculated rcond(A)'s to be 0.019 and 0.040 for polarimetric sensors and 0.16 for an elliptical core fiber sensor [22,23]. From the experimental results a rcond(A) of 0.23 was obtained, which means that the system of equations is well-conditioned.

Even though this system of equations has a good condition number, the range in which both strain and temperatures can be measured simultaneously is limited to only 10- 20 °C. Perhaps future research can identify fluids that will allow for a greater range of temperatures in which strain and temperature can be measured simultaneously.

7.0 Liquid Core Fibers for Cooling

Liquid core fiber sensors can be utilized for the purpose of measuring strain and temperature as was described previously and for the purpose of material cooling. In order to demonstrate that liquid core fiber sensors could be used for cooling an experiment, with the setup shown in Figure 7.1 was devised. The water reservoir was pressurized to 20 psi, using a pressure pump, so that water would flow through 120 cm of 550/670 μm hollow core fiber. A 9 cm section of the hollow core fiber was surrounded by water. A hot plate was used to slowly increase the surrounding temperature of the 9 cm section of fiber, which was monitored with a mercury thermometer. A thermocouple was used to monitor the temperature of the water emerging out of the end of the hollow core fiber.
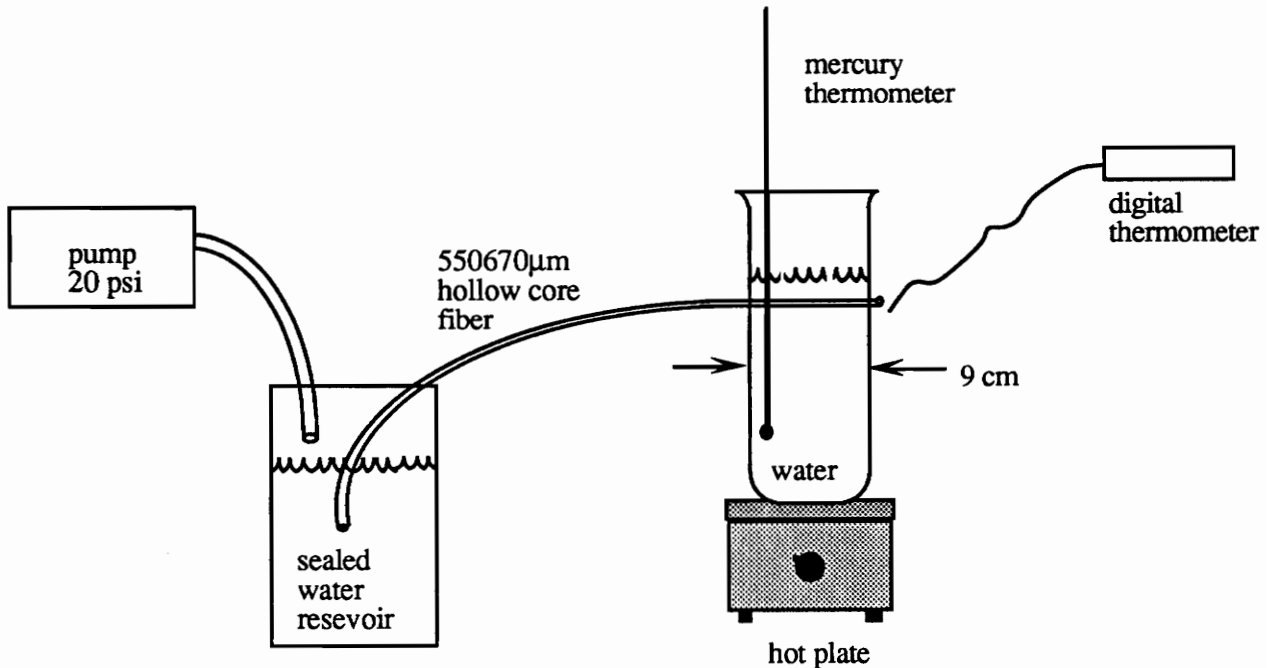

Figure 7.1. Experiment to investigate the possibility of using liquid core fibers for cooling.

In order to determine whether there was any temperature increase due to friction, the pump was turned on and the water reservoir temperature was compared to that of the water coming out of the hollow core fiber. No difference in temperature was observed, indicating that no measurable temperature changes occur due to frictional effects alone.

The temperature of the water surrounding the hollow core fiber and the temperature of the water coming out of the end of the hollow core fiber were monitored, while slowly increasing the temperature of the hotplate. A flow rate of 0.7m/sec was maintained during the first experiment. During the second experiment the water was allowed to slowly drip out of the end so the flow rate was very low. The results in Figure 7.2 indicate that at a flow rate of 0.7m/sec, the water in the liquid core fiber was not able to reach the temperature of the thermal bath in the time needed for its flow through the fiber. At the drip rate the output temperature of the water more closely approached the temperature of the surrounding bath. This means that more heat is transferred to the water in the fiber at the drip rate than at the flow rate of 0.7m/sec.
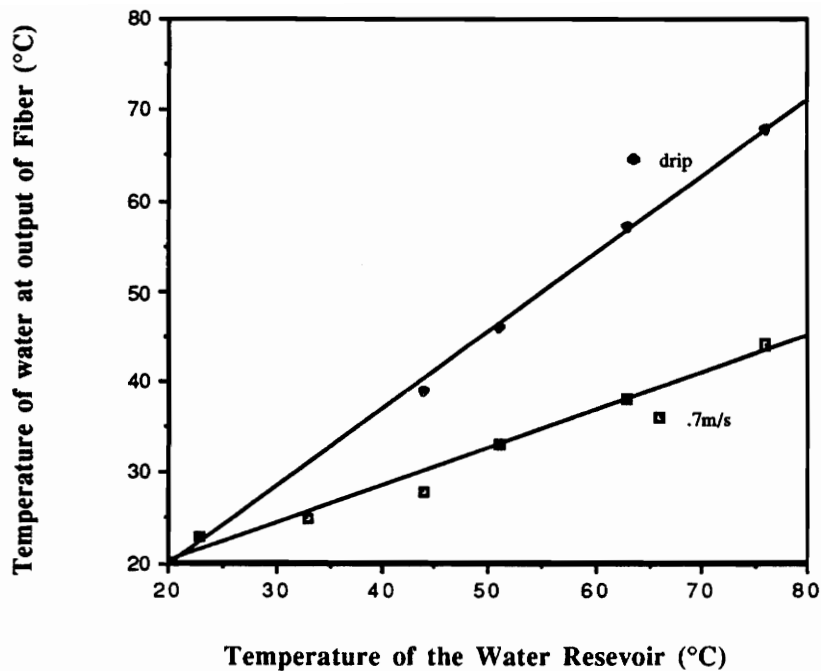
Figure 7.2. Results of ambient temperature vs. temperature in the fiber.

In Figure 7.2, we see that for a surrounding temperature of 76 °C, an inlet temperature of 23 °C, an effective heating length of 9 cm and a flow rate of 0.7 m/sec, the temperature of the water emerging from the fiber is 44 °C. This demonstrates that liquid core fibers can be used for cooling.

7.1 Liquid Core Fiber Coupler Development

In order to pump a liquid through the hollow core fiber, while also being able to inject light into the hollow core fiber, special liquid core to solid core fiber interfaces were designed.

7.1.1 Solid Core to Liquid Core Fiber Interfacing Technique I

Solid-core to liquid-core couplers were made by sandwiching a curved fiber between two microscope slides and polishing the sandwich to expose the core of the fiber. These couplers utilized 403/483 μm solid core glass optical fiber and 540/670 μm hollow core fiber as the liquid core fiber. By injecting light from a helium neon laser into the solid-core fiber, the output power out of both the solid-core and the liquid-core fiber could be measured. From these values, the splitting ratios between the two outputs could be calculated. The power input to the coupler is approximated by cutting back the input fiber between the source and the coupler. Since the loss incurred in the short length of fiber is negligible, measurement of the power out of this short length gives a good approximation of the power input to the coupler. The coupler demonstrated an excess loss of 9.3 dB and a splitting ratio of 80/20 (solid-core output to liquid-core output). Close examination of this coupler revealed that after polishing, alumina grit from the polishing pad had been deposited inside the hollow core fiber, and this opaque grit was responsible for the high losses. Techniques for thoroughly cleaning the hollow core fiber after polishing will need to be developed in the future if this kind of a coupler is desired.

7.1.2 Solid Core to Liquid Core Interfacing Technique II

A coupler technique was also developed in which the solid core fiber was physically inserted into the side of a hollow core fiber. In this procedure, the liquid core fiber is sandwiched between two glass slides, and polished to expose the core, as before. When the hole into the core is sufficiently large, the solid-core fiber is inserted into the opening, see Figure 7.3. The opening is then sealed with epoxy. These couplers have less loss than the couplers described in the previous section yet alumina grit still contaminates the liquid core fiber.
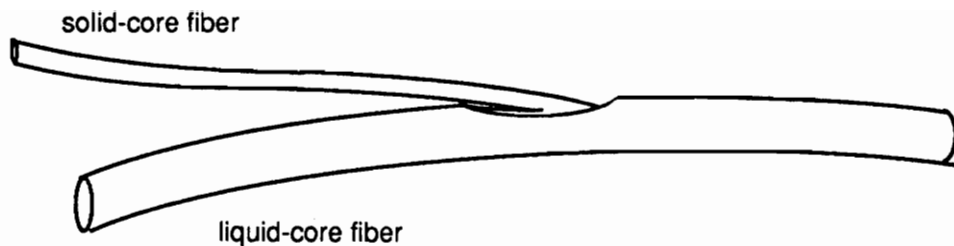
solid-core fiber

liquid-core fiber

Figure 7.3. Solid-core to liquid-core coupler design.

7.1.3 Solid Core to Liquid Core Interfacing Technique III

In this technique a 100/125 μm multimode fiber is inserted into a 550/670 μm liquid core fiber as is shown in Figure 7.4. The liquid core fiber and the multimode fiber are both epoxied to a glass slide. Since the multimode fiber is only 125 μm in diameter, and the inner diameter of the hollow core fiber is 550 μm, liquid can still be pumped through the hollow core fiber, by placing the whole coupler in the cooling fluid.

solid core fiber

liquid core fiber

epoxy

glass slide

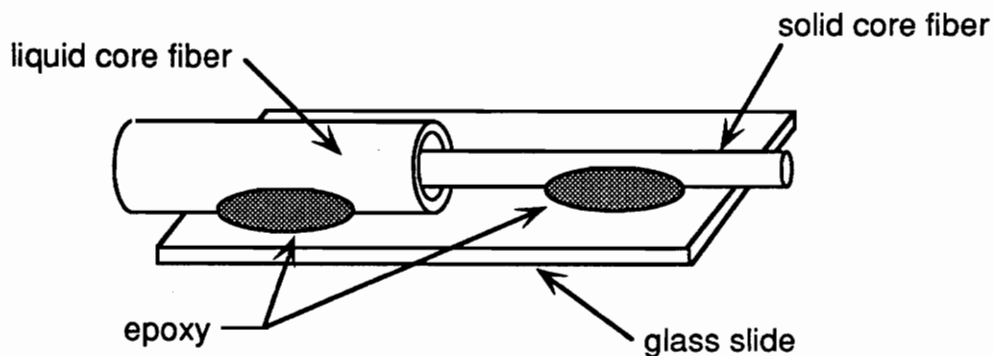Figure 7.4. Light coupling from solid to liquid core fiber.

The feasibility of this coupler approach was investigated by injecting 580 μW of light into the multimode fiber and observing 20 μW of light at the output end of the fiber, with another multimode fiber. This represents an insertion loss of 15 dB, most of the loss can be attributed to the mismatch in cores between the solid core and liquid core fiber.

Finally this liquid core fiber was connected to the OTDR, in a setup similar to the one shown in Figure 3.1. The temperature of the liquid core fiber was increased by taping the liquid core fiber to a hot plate and slowly increasing the hotplate temperature, while a pressure pump was used to pump silicone fluid through the fiber. The results of this test with the pump on and off are shown in Figure 7.5. These results show that a liquid core fiber can be used to measure temperature while liquid is being pumped through it. This coupler has been shown to be the most effective way to couple light into the liquid flowing through the fiber. By choosing a solid core optical fiber, at the output, with a larger core radius more light can be coupled into the fiber.

$y = 7.8938 - 0.29658x$ $R^2 = 1.000$ ● rel ps pump on
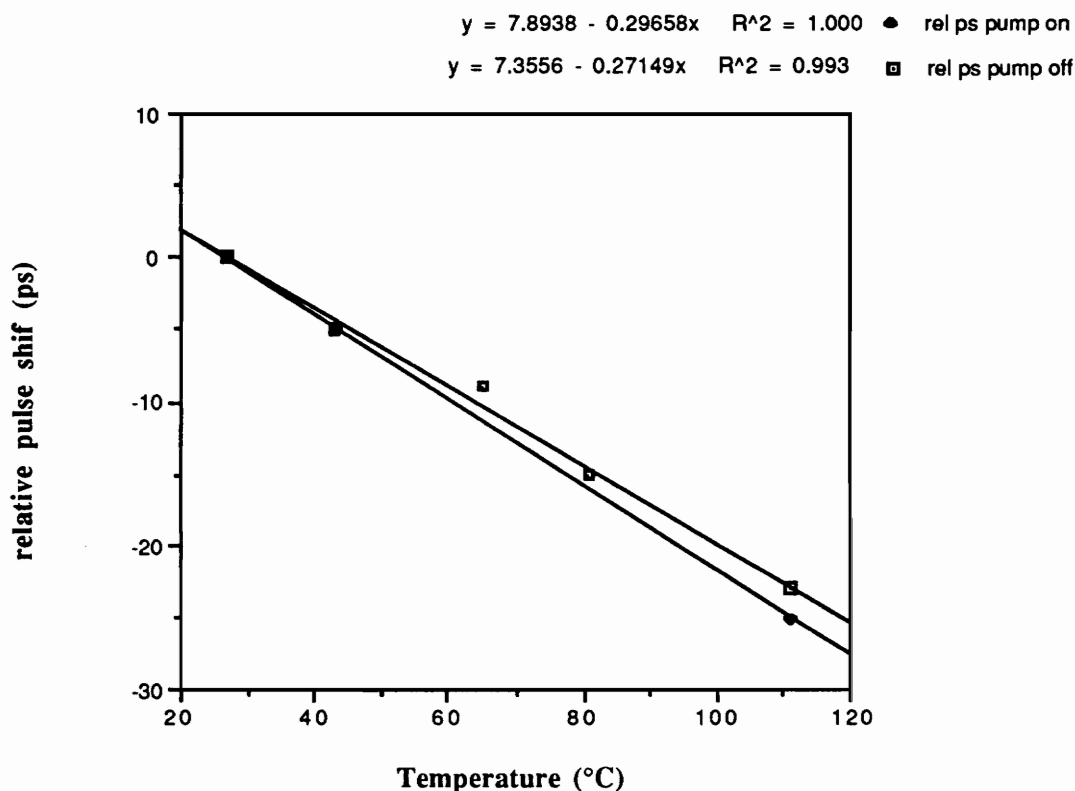$y = 7.3556 - 0.27149x$ $R^2 = 0.993$ ▫ rel ps pump off

Figure 7.5. Temperature versus average pulse shift for pump on and off conditions.

8.0 Conclusion

In this thesis we have demonstrated that liquid core fibers can be used for measuring strain and temperature simultaneously by monitoring both the intensity of an optical pulse and the optical time delay of the pulse using OTDR techniques. We have given a background on the uses of liquid core fibers for both sensing and communication applications and described in detail how liquid core fibers are manufactured. A theoretical model was developed to predict the time delay of an optical pulse in a fiber as it was strained or heated and an evanescence-based theory was also developed to predict the drop in intensity with increase in temperature. These theoretical models were then experimentally verified.

In order to monitor strain and temperature simultaneously a linear system of equations with four unknown coefficients was evaluated. The four constants were experimentally determined to resolve the temperature and strain in the sensing system. In order to determine whether the system of equations is sensitive to small changes in the observed optical time delay or intensity the condition number was determined, for the four coefficients in the equations. A reciprocal condition number of 0.23 was determined; i.e. a small change in the observed time delay or drop in intensity does not affect the predicted value for the temperature and strain much, the equations are well-conditioned.

In order to demonstrate that the liquid core fibers could also be used for cooling purposes, while also being able to measure temperature, silicone oil was pumped through a hollow core fiber while monitoring the time delay of an optical pulse on the OTDR.

Even though we have demonstrated, in this thesis, that strain and temperature can be measured simultaneously using OTDR techniques and that the system of equations are well-conditioned, we are still limited to a sensing region of 10 to 20 °C. Perhaps future research can identify fluids that will allow for a greater range of temperatures in which strain and temperature can be simultaneously measured.

References

1. J. Dakin and B. Culshaw, 1988. Optical Fiber Sensors: Principles and Components, Artech House, Boston, MA.

2. J. Stone, 1972. "Optical transmission in liquid core quartz fibers," Applied Physics Letters, 20, pp 239 - 240.

3. G.J. Ogilvie, R.J. Esdaile and G.P. Kidd, 1972, "Transmission Loss of Tetracholoroethylene-filled liquid-core-fibre light guide," Electronic Letters, 22.

4. D.A. Pinnow, T.C. Rich, F.W. Ostermayer, M. DiDomenico, "Fundamental optical attenuation limits in the liquid and glassy state with application to fiber optical waveguide materials," Applied Physics Letters, Vol. 22, No. 10, 15 May 1973.

5. D.N. Payne and W.A. Gambling, 1972, "New low-loss liquid core fibre waveguide," Electronic Letters, 8 pp. 374 - 376.

6. M. Kuribara and Y. Takeda, 1983. " Liquid core optical fiber for voltage measurement using Kerr effect," Electronic Letters, 19, pp. 133 - 135.

7. A.H. Hartog, 1983. "A distributed temperature sensor based on liquid-core optical fibers," Journal of Lightwave Technology, LT - 1, pp. 498 -509.

8. A.H. Hartog, "Variation of pulse delay with stress and temperature in jacketed and unjacketed optical fibres," Optical and Quantum Electronics, 11, 1979, pp. 265 - 273.

9. S.J. Huard, C.Viossat-Thomas, "A New Optical Fiber Temperature Sensor using Paraffins for Medical Application," SPIE, Vol. 1011, Fiber Optic Sensors III, 1988.

10. E.A. Soares, T.M. Dantas, "Bare Fiber Temperature Sensor," SPIE, Vol. 1367, Fiber Optic and Laser Sensors VIII, 1990.

11. Cargille, Specialty Optical Liquids Catalog, Cargille, Cedar Grove, NJ 07009.

12. B. Zimmerman, R. Claus, M. Gunther, J. Greene, M. de Vries, "A Novel Liquid Core Fiber Temperature Sensor For Smart Structure Applications," Journal of Intelligent Material Systems and Structures, Vol. 1, #1, Jan 1990.

13. B. Zimmerman, R.O. Claus, D.A. Kapp, K.A. Murphy, "Fiber Optic Sensors Using High Resolution Optical Time Domain Instrumentation Systems," Journal of Lightwave Technology, vol. 8, no. 9, pp. 1273-1277, Sept. 1990.

14. B. Zimmermann, R. Claus, "Recent Progress in Optical Time Domain Techniques," Proceedings of the Conference on Optical Fiber Sensor-Based Smart Materials and Structures, April 3-4, 1991, pp. 13.

15. B.D. Zimmermann, "High Resolution Optical Time Domain Reflectometry and its Applications," Masters Thesis, January 19988, Virginia Polytechnic Institute and State University.

16. M. R. Brininstool, "Measuring longitudinal strain in optical fibers," Optical Engineering, November 1987, Vol. 26, No. 11, pp. 1112 - 1119.

17. D.C. Gloge, "Weakly guiding fibers," Applied Optics, pp. 2442 - 2451, 1971.

18. M.J. de Vries, B.D. Zimmermann, A.M. Vengsarkar, R.O. Claus, "Liquid Core Optical Fiber Temperature Sensors," Proceedings of the Conference on Optical Fiber Sensor-Based Smart Materials and Structures, April 3-4, 1991, pp. 182.

19. M.J. de Vries, B.D. Zimmermann, A.M. Vengsarkar, R.O. Claus, "Liquid Core Optical Fiber Temperature Sensors," IEEE Southeastcon conference, Williamsburg, April 1991.

20. Atkinson K., Elementary Numerical Analysis, Chpt. 8, John Wiley & Sons, 1985.

21. Burden R.L., Numerical Analysis Fourth Edition, Chpt. 7, PWS-Kent, 1988.

22. Z. G. Wang, "Simultaneous Measurement of Strain and Temperature using Two-Mode Elliptical Core Optical Fiber," Masters Thesis, June, 1992, Virginia Polytechnic Institute & State University.

23. A.M. Vengsarkar, W.C. Michie, L. Jankovic, B. Culshaw, R.O. Claus, "Fiber Optic Dual-Technique Sensor for Simultaneous Measurement of Strain and Temperature," Proc. SPIE, Vol 1367, pp. 249 - 260, 1990.

Marten de Vries was born on May 20, 1965 in Novara, Italy, and is a citizen of the Netherlands. He received his secondary education at the Revius Lyceum in Doorn, the Netherlands. He completed his Bachelor of Science Degree in Electrical Engineering at Virginia Polytechnic Institute and State University in December 1989. He was a cooperative education student with Litton Polyscientific in Blacksburg, VA and General Electric in Salem, VA. He received his Master's Degree in Electrical Engineering in January 1993. He held positions as a graduate research assistant and as a graduate project assistant . He is a member of the Institute of Electrical and Electronic Engineers, the International Society for Hybrid Microelectronics and is the president and founder of the student chapter of the Optical Society of America at Virginia Tech.

Marten speaks English, Dutch, German, Italian and French (in order of proficiency). He enjoys many different sports, such as tennis, rugby, speedskating and rockclimbing.